Honors Theses

5-2018

Investigating Stainless Steel Particle Synthesis

Michael E. Klaczko

Follow this and additional works at: https://digitalcommons.esf.edu/honors

Part of the Materials Chemistry Commons

Investigating Stainless Steel Particle Synthesis
by

Michael E. Klaczko
Candidate for Bachelor of Science
Chemistry
With Honors

May 2018

APPROVED

Thesis Project Advisor: _____
Mathew Maye, Ph.D.

Second Reader: _____
Kelley Donaghy, Ph.D.

Honors Director: _____
William M. Shields, Ph.D.

Date: _____

Abstract

This thesis focuses on the chemistry for stainless nanoparticle synthesis in order to develop corrosion resistant nanoparticles. Syntheses within the Maye lab have been successful, however at the large scale these processes have been hindered by low yields as a result of byproduct formation and oxidation loss. This study addresses these problems by introducing a new precursor to synthesize the Fe core of FeCr/Ni stainless core/shell particles. Traditionally iron pentacarbonyl ($Fe(CO)_5$ is used, but this study uses iron acetylacetonate ($Fe(acac)_3$) as a substitute. Although the degradation of $Fe(CO)_5$ is more commonly used and is understood relatively well, $Fe(acac)_3$ is safer and less costly. Properly synthesized particles show high crystallinity and have immense magnetic capabilities. A comparison between the two precursors is completed in this work. The ability for Fe^0 particles to act as a core for stainless particles and the effects of shells on the cores is also analyzed. Analysis of the particles was done using thermogravimetric analysis (TGA), Laser Ablation Induced Coupled Plasma Mass Spectrometry (LA-ICP-MS), Physical Property Measurement System (PPMS), and x-ray diffraction (XRD). These analysis methods allow for the approximate composition of the particles to be determined and the approximate extent of oxidation to be estimated. Results of the study show that $Fe(acac)_3$ iron particles are less metallic than $Fe(CO)_5$, suggesting that $Fe(acac)_3$ is not an effective substitute for $Fe(CO)_5$. This shows that further research needs to be completed in order to find a potential substitute or create a new route for the successful creation of stainless nanoparticles.

Table of Contents

Abstract

Table of Contents

Acknowledgements

Introduction

Transition metal oxide nanoparticles have gained significance in the materials field because of their ability to exhibit the desired characteristics of regular metal nanoparticles with greater durability. Magnetism, conductivity, and high strength are all found to varying degrees within nanoparticles composed of transition metal oxides[1-3]. Stainless nanoparticles enhance these characteristics by adding the ability to resist corrosion and oxidation thus increasing their lifetime and broadening their capabilities by preserving metal properties[4]. The abilities of these nanoparticles rely on their composition and morphology which makes them easily adaptable. Such adaptability allows for these particles to be tailored for use, further idealizing utilization in their respective applications[5-7]. Iron (Fe) nanoparticles have become some of the more popular metal nanoparticles to study because of their massive magnetic capabilities. Currently these particles are used in bioseparation, *in situ* drug delivery, biosensing, and as imaging contrast agents[5-8].

To successfully synthesize metallic Fe nanoparticles with high magnetism, specific controlled reactions need to be done in order to prevent them from oxidizing. Iron readily reacts with oxygen in any form and creates different iron oxides. This is especially true at the nanoscale where iron nanoparticles have an incredible surface area to volume ratio. To counter oxidation, one study has been done to determine how iron particles oxidize and their rates of oxidation[4]. While iron nanoparticle oxidation is not completely understood, it has been found that using specific precursors and organic solvents can lead to minimal amounts of particle loss to oxidation.

In order to successfully synthesize iron nanoparticles a suitable iron precursor must first be picked to maximize irons metallic characteristics. Research has been done on maximizing these characteristics revealing that various precursors offer different advantages over others[9]. As discussed in Mendoza-Garcia and Sun, $Fe(CO)_5$ has been identified as a precursor which produces stabile and strongly magnetic iron nanoparticles identifying it as a top choice for magnetic iron particle synthesis and as a stainless nanoparticle core[10]. Not only does it provide ideal particles, but its thermal decomposition has been studied extensively and is well understood[11,12].

Syntheses can be done in aqueous solutions, but oftentimes these particles oxidize quickly or have low magnetism[10]. To control the synthesis of Fe nanoparticles, organic solvents are used[13-15]. When using $Fe(CO)_5$ it is often dispersed in high boiling point solvents which prevent the iron particles from oxidizing. To control the size of the synthesized nanoparticles, oleylamine and hexadecylammmonium chloride (HDACL) are added to the solution. In Boles et al. it has been shown that the presence of more ligands in a reaction mixture creates smaller nanoparticles and ligands in general play a large role in the surface chemistry of the particles[16]. In Zhang et al., it was shown that halides also play a strong role in controlling nanoparticle growth as the halides strongly bond to the $Fe(CO)_5$ molecules[17]. The presence of Cl^- from the HDACl therefore limits the growth of the nanoparticles and contributes to the creation crystalline iron nanoparticles.

Structurally, iron nanoparticles follow various phenomena to form many different structures. Studies have shown that often metal nanoparticles form nanocrystals and their structures change based upon their composition and how they are synthesized[18,19]. As discussed in Bai et al., nanoparticles often form hollows structures through processes

such as the Kirkendall Effect, Ostwald Ripening, and Galvanic exchange[20]. These so called self-templating processes develop from a difference in diffusion rates of the different metals present in the nanoparticles[20]. Other studies support these findings and describe how these phenomena can be taken advantage of to tailor the structure of iron nanoparticles for specific application[21-23]. Following the aforementioned synthesis with $Fe(CO)_5$ in octadecene in the presence of both oleylamine and HDACl, body centered cubic nanoparticles are formed[24-26]. Ligands on the surface of the particle can be exchanged which allows the particles to become more stable or functionalized[27]. Once stable metallic iron particles are developed, they can be used as the core of bimetallic or alloy core/shell nanoparticles for purposes of further stabilization or to add oxidation resistance as is the case with stainless nanoparticles.

To make iron nanoparticles stainless, chromium and nickel can be deposited as a shell onto the iron particles turning them into the cores of core/shell nanoparticles. While similar techniques have been used before, this unique technique combines the properties of both components into one system creating a stainless particle[28,29]. With a shell comprised of chromium and or nickel, the iron particles are protected from oxidation and therefore become stainless. Berlia et al. determines the high corrosion resistance capabilities of particles coated with these metals[30]. While the addition of the shell material imbues this characteristic on the iron particles, it also changes their morphology and reactivity. The effects of the addition of various metals is beginning to be studied especially with iron core particles with nickel or chromium shells[30-34]. While it has been found that iron nanoparticles have the potential to fulfill new applications and enhance

old ones, the syntheses of the particles have begun to be scrutinized for their low yield and cost.

Although stainless iron nanoparticle syntheses are successful, the processes used to create them have a low yield and use hazardous and costly precursors. In an attempt to address this, the precursor $Fe(acac)_3$ is used in this study in place of $Fe(CO)_5$ to synthesize Fe^0 cores. The molecule has a similar structure and the former is much cheaper and safer than the latter. The major difference with $Fe(acac)_3$ in iron nanoparticle synthesis is that it must be reduced from its Fe^{3+} state to Fe^0. This was done by adding 1,2-dodecandiol when the reaction mixture is at high temperatures. For comparison, iron cores were synthesized using both precursors. Chromium and or nickel were deposited onto iron cores synthesized with $Fe(CO)_5$. All syntheses products were analyzed with XRD to determine their composition. All products were also measured via TGA to determine approximate composition. LA-ICP-MS was used to support the XRD results found on the iron particles synthesized from $Fe(CO)_5$ and to determine the composition of the supernatant from these syntheses. PPMS was also done on these particles to determine their magnetism.

Methods based on the procedure outlined in Pathade et al, 2016[4]

Materials

Iron (0) pentacarbonyl ($Fe(CO)5$, 99.5%), (bistriphenyphosphine) dicarbonyl nickel (0) ($Ni(CO)2(PPh3)2$, 98% anhydrous), chromium (0) hexacarbonyl ($Cr(CO)6$, 99%), Iron (III) acetylacetonate ($Fe(acac)_3$, 97%), oleylamine (OAm, 70%), 1-octadecene (ODE, 90%), Oleic Acid (OAc, 90%), Benzyl ether (($C_6H_5CH_2)_2O$, 98%), 1,2-dodecanediol ($CH_3(CH_2)_9CH(OH)CH_2OH$, 90%), and ethanol (EtOH, 200 proof) were

purchased from Sigma-Aldrich and used without further purification.

Hexadecylammonium chloride (HDACl) was synthesized from HDA.

Fe^0 Particles from Fe(CO)$_5$

Stainless steel nanoparticles were synthesized from the thermal degradation of
Fe(CO)$_5$. This was done by creating a mixture of 20 mL of ODE, 200 mg of HDACl, and
2 mL of OAm which was degassed for 1 hour at 120 °C. This mixture was then heated to
180 °C under argon. Once at temperature 1 mL of Fe(CO)$_5$ was injected into the system
using a metal syringe. This mixture was constantly agitated by shaking the apparatus as it
was annealed at 180 °C for an hour.

Fe^0 Particles from Fe(acac)$_3$

Similar to the synthesis of the Fe^0 particles from Fe(CO)$_5$, Fe^0 particles were
synthesized from the thermal degradation of Fe(acac)$_3$. This was done by mixing 20 g of
Fe(acac)$_3$, 500 mL of benzyl ether, 60 mL of OAc, and 60 mL of OAm. This mixture was
heated to 200 °C 1 hour. While heating, 10 g of 1,2-dodecandiol was dissolved in 40 mL
of benzyl ether with heat. This was added to the reaction mixture after heating was
finished and the mixture was heated to 220 °C. This mixture was heated at this
temperature for 2 hours.

FeCr, FeNi, FeCrNi, and FeNiCr Particles

For Cr shells, 650 mg of Cr(CO)$_6$ and 200 mg of HDACL were dissolved in 20
mL of oleylamine with heating at inert atmosphere. This mixture was added in equal
portions into the main Fe(CO)$_5$ mixture to keep the temperature of the mixture around
220 °C until it was all gone. Ni shells were prepared similarly by dissolving 1.5 g of
Ni(CO)$_2$(PPh$_3$)$_2$ and 200 mg of HDACL in 20 mL of oleylamine with heating at inert

atmosphere. This mixture was also added in equal portions into the main $Fe(CO)_5$

mixture to keep the temperature of the mixture around 220 °C until it was all gone. To

synthesize a particle with a Cr/Ni alloy shell, the same procedure is followed with both

precursors being dissolved in the shell mixture in a desired ratio.

Nanoparticle Purification

Cleaning of any synthesized particles was done by precipitating the product with

ethanol. Using a 1:3 particle to ethanol volumetric ratio, particles were centrifuged at

4000 RPMs for 15 minutes. This was repeated until the particles were no longer oily,

often coming clean after 2 cycles of cleaning. Each cleaning cycle ended by decanting the

ethanol mixture off of the particles. Depending on how the particles were stored, they

were either re-dispersed in a suitable volume of hexane or toluene or were left open to the

atmosphere to dry into a powder.

Instrumentation

All LA-ICP-MS data was gathered on a New Wave UP193 Laser Ablation unit

(SUNY ESF, Baker Hall, Syracuse, NY). Each sample was mounted on a petrographic

slide after being deposited on carbon black and pressed into a pellet. During analysis the

sample is ablated with a solid-state pulse laser beam and the resulting vapor is transported

into the 8000 K argon plasma. Once ionized from the plasma, the ions are analyzed by a

mass analyzer and are separated according to their mass charge ratio. Magnetism

measurements were made using a Quantum Design Physical Property Measurement

System, or PPMS (Cornell University, Cornell Center for Materials Research). Using a 9

Tesla superconducting magnet in a helium dewar, samples were placed on a sample rod

and their magnetic response was measured through two pickup coils. XRD measurements

were taken via a Bruker D8 Advance powder diffractometer using Cu Kα radiation. The diffraction angles were scanned over 25-60° in search of specific metallic peaks. Samples were placed onto a zero-diffraction silicon dioxide crystal with tape, gel, or through drop casting based upon the particle medium. TGA measurements were taken on a PerkinElmer Pyris1 TGA using a thermal analysis gas station under a O_2 purge. Samples were heated from 50 °C to 800 °C at a rate of 10 °C/min. Samples were drop cast and their solvents were dried at standard conditions or in a speed vac.
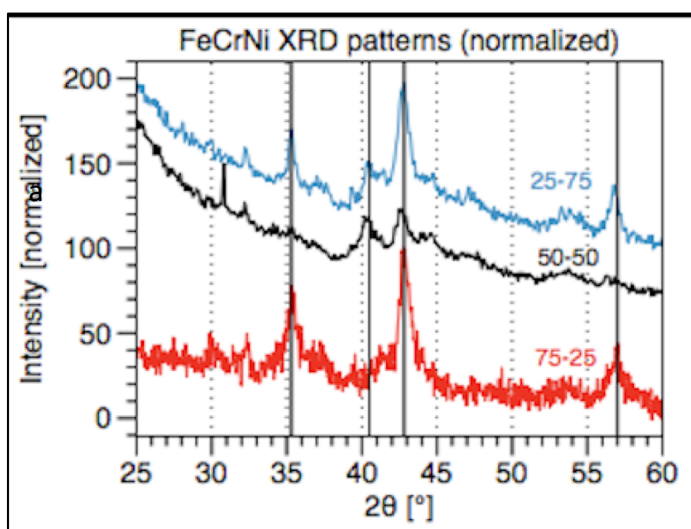
Results and Discussion

Figure 1: XRD analysis of FeCrNi nanoparticles using iron core synthesized from $Fe(CO)_5$ (data from Dr. Mathew Maye)

The effectiveness of $Fe(acac)_3$ was shown to be equivalent in comparison to $Fe(CO)_5$. Both precursors underwent similar processes and had similar results, therefore showing seemingly no substantial advantage over $Fe(CO)_5$. Analysis did reveal that the iron particles synthesized from $Fe(acac)_3$ were more extensively oxidized than those from $Fe(CO)_5$. Figure 1 shows that particles synthesized from $Fe(CO)_5$ showed an M_3O_4 (M = Fe, Ni, Cr) oxidation peak at about 35.1°. Figure 2 shows that particles synthesized from $Fe(acac)_3$ have this peak and a second M_3O_4 (M = Fe, Ni, Cr) peak at around 29.8°. Both samples also show M_3O_4 (M = Fe, Ni, Cr) oxidation peaks at about 57°. Figure 2 shows that the particles synthesized from $Fe(acac)_3$ show another M_3O_4 (M = Fe, Ni, Cr) oxidation peaks at about

53°. In addition, Fe^0 metallic iron is seen at about 42.9° in both samples but is seen with much less intensity in the Fe(acac)$_3$ iron particles. This suggests that the particle is less
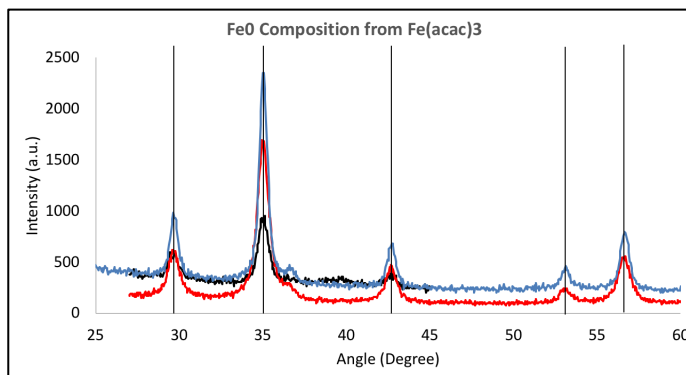

Figure 2: Fe^0 nanoparticles synthesized from Fe(acac)3.

metallic most likely due to loss of metallic iron to oxidation. Altogether the XRD data shows that the particles synthesized with the Fe(acac)$_3$ precursor were less metallic and more oxidized than the particles synthesized from the Fe(CO)$_5$ precursor. Reasons as to why this happened point to the possible inability of iron nanoparticles to form in a crystalline bcc configuration when made from Fe(acac)$_3$. While these particles show similar bcc XRD peaks, the structures may not have been fully developed and therefore could have been left susceptible to oxidation. The majority of the oxidation shown in these particles can most likely be attributed to the oxygen present in solution. Some oxidation of the particles can also be attributed to the reaction of the particles to oxygen in the atmosphere. This problem would be mitigated by depositing a shell on the particles, but the inadequate core particles formed from these syntheses were not deemed sufficient enough to warrant the deposition of a shell onto them. Regardless of how the particles get oxidized, the XRD data shows that when oxidized the iron particles conclude at the Fe$_3$O$_4$ stage.
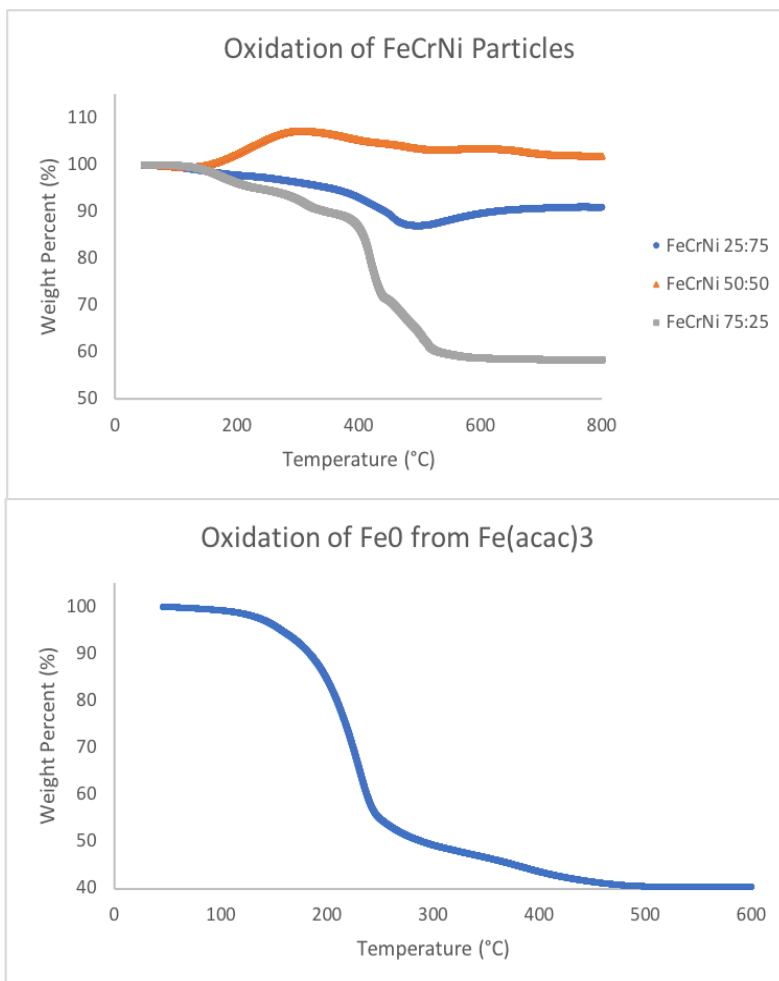
Figure 3: TGA of both a) FeCrNi particles synthesized using Fe_0 cores made from $Fe(CO)_5$ and b) Fe^0 particles synthesized using $Fe(acac)_3$

The oxidation of $Fe(CO)_5$ is attributed to reactions with oxygen in the atmosphere almost completely. Because the iron from $Fe(acac)_3$ is oxidized, the extent of iron oxidation is due to lack a reduction by the reducing agent. To compare the extent to which the two different iron particles were oxidized, TGA was done on each set of particles.

Figure 3 shows that when the particles that utilized the Fe^0 core from $Fe(CO)_5$ were analyzed up to 800 °C, they showed mass gain in two distinct parts of their analysis. This is evidence of the process of oxidation as the addition of oxygens to the iron particles will increase their mass. Overall mass loss is attributed to the loss in organic materials such as ligands and excess solvent being burned off of the particles. The first increase in mass around 250 °C is attributed to irons oxidation into Fe_2O_3. The second mass gain shown around 600 °C can be attributed to the further oxidation of the Fe_2O_3 to Fe_3O_4. While both of these mass gains are present in the particles synthesized using $Fe(CO)_5$, neither of

thse peaks are seen in the analysis of the particles made from Fe(acac)$_3$. This would suggest that the particles made from Fe(acac)$_3$ were already fully oxidized and therefore were unable to oxidize further and gain mass. This again supports the use of Fe(CO)$_5$ as a precursor for the synthesis of Fe^0 as it is shown that the synthesized particles are mostly unoxidized and metallic.

The particles loss that result from the use of Fe(CO)$_5$ seem to be attributed to the reaction of iron ions with the ligands or solvent present in the reaction mixture.
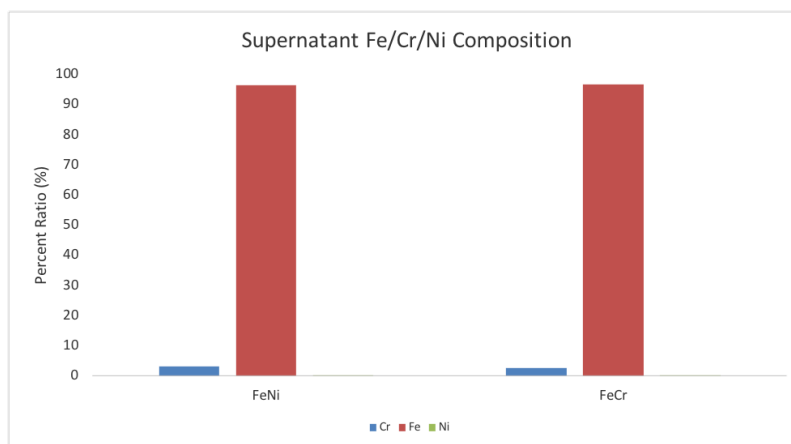

Figure 4: LA-ICP-MS data showing the amount of iron, nickel, and chromium in the supernatant of a reaction mixture for each respective particle

This result was determined after analyzing the composition of the supernatant of a FeNi reaction and a FeCr reaction. Figure 4 shows the amount of iron, nickel, and chromium present in the supernatant of the reaction mixture of both FeCr particles and FeNi particles through LA-ICP-MS analysis. For each synthesis there was little to no shell material found in the supernatant. Instead, very high amounts of iron were present showing that the missing iron nanoparticle product was being lost to the supernatant. This supports the idea that iron is lost to the ligands or solvent in the reaction mixture, most likely being taken up in aggregates or complexes before reaching the desired Fe^0 state.

To ascertain that the deposition of the chromium and nickel shell material was successful, LA-ICP-MS was also used to analyze the composition of the FeCr and FeNi
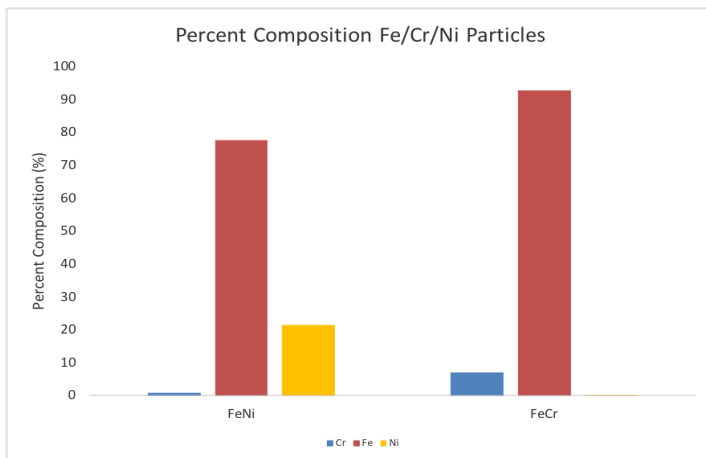
Figure 5: Analysis of FeNi and FeCr particles using LA-ICP-MS shows that each set of particles contained their respective core and shell materials

synthesized particles. Figure 5 shows the amount of iron, nickel, and chromium present in each set of both FeCr particles and FeNi particles. For the FeNi particles, about 75% of the particle was comprised of iron and 25% of the particle was comprised of nickel. The FeCr particles were composed of about 90% iron and 10% chromium. This data therefore shows that shell deposition is working successfully on the iron particles. The data also shows that more nickel is being deposited on the iron cores than chromium. Because there was no nickel or chromium found in the supernatant it can be determined that this must have to do with the available amount of iron in each synthesis. The higher ratio of iron to chromium in the FeCr particles would suggest that less iron particles were lost to the supernatant in this synthesis than in the synthesis of the FeNi particles.

To determine if the iron particles synthesized using $Fe(CO)_5$ were actually magnetic and are able to maintain their magnetism with a stainless shell on them, PPMS was done on synthesized FeCrNi particles. Figure 6 shows the magnetic data that was gathered from this analysis which shows differing strengths of magnetism for the particles. This data indicates that the shell material effects the particles magnetism, as different ratios of Ni and Cr seemed to weaken the magnetism of the particles. When the ratios of the two shell materials were equal, the magnetism of the particles were more

than double that of the particles where the ratio of Cr or Ni to the other is 1:3. Both sets of particles that had this ratio had similar magnetism values no matter which particle held the majority. This would
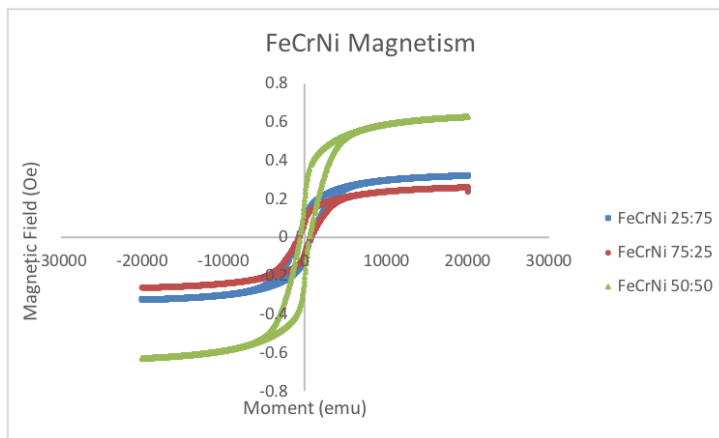

Figure 6: Magnetism data for three samples of FeCrNi particles with varying ratios of shell material

suggest that an imbalance in shell material causes an interference with the magnetism of the iron core. Despite their differences in magnetic strength, all three of the particles exhibited hysteresis which is shown by the hysteresis loops within Figure 6. This is directly attributed to the ferromagnetic properties of iron. Further studies must be done to better understand the effects of shell structures on a particles magnetism, as this directly effects the ability of stainless particles to be magnetic.

Conclusion

Overall it seems that $Fe(acac)_3$ is not as effective as $Fe(CO)_5$ when synthesizing Fe^0 nanoparticles. Thus far there have been little to no advantages of using the precursor as it actually creates less metallic particles. $Fe(CO)_5$ was proven to synthesize metallic Fe^0 nanoparticles but only with loss of iron to the reaction mixtures supernatant. The particles that the precursor does create are highly magnetic and unoxidized. While it has been determined that particles are lost to the supernatant of the reaction, it seems that the shell precursors are impervious to this problem. The study has also shown that the deposition

of shell material onto iron cores can be successfully done, but the addition of different ratios of shell material change the magnetism of the particles overall.

Future work could be done to further study the effects of adding shell material to nanoparticles. This is especially important for particles such as iron nanoparticles which have great potential for widespread applications but a weakness to oxidation. Specific shells need to be researched which can be used without greatly hindering the advantageous characteristics of the core material. If particles are to be made stainless their characteristics much first be unaltered. Further research can also be done into finding another precursor to use in place of $Fe(CO)_5$ or to design a completely different more cost effective and safe synthesis route altogether. Once these techniques are determined, the finer details of metal oxidation can be scrutinized and potentially avoided altogether. The results of this research show that the potential for this technology is there, but much work still needs to be done in order for the technology to be widely implemented.

References
1. Jain, P. K.; Huang, X.; El-Sayed, I. H.; El-Sayed, M. A. Plasmonics 2007, 2 (3), 107–118.
2. Sonvico, F.; Dubernet, C.; Colombo, P.; Couvreur, P. Current Pharmaceutical Design 2005, 11 (16), 2091–2105.
3. Li, X.; Zhao, T.; Sun, L.; Aifantis, K. E.; Fan, Y.; Feng, Q.; Cui, F.; Watari, F. Journal of Biomedical Materials Research Part A 2015, 104 (1), 322–339.
4. Pathade, L.; Doane, T.L.; Slaton, R. D.; Maye, M. M. Journal of Physical Chemistry C 2016, 120 (38), 22035-22045.
5. Lee, J.-H.; Huh, Y.-M.; Jun, Y.-W.; Seo, J.-W.; Jang, J.-T.; Song, H.-T.; Kim, S.; Cho, E.-J.; Yoon, H.-G.; Suh, J.-S.; Cheon, J. Nature Medicine 2006, 13 (1), 95–99.
6. Neuberger, T.; Schöpf, B.; Hofmann, H.; Hofmann, M.; Rechenberg, B. V. Journal of Magnetism and Magnetic Materials 2005, 293 (1), 483–496.
7. Gupta, A. K.; Gupta, M. Biomaterials 2005, 26 (18), 3995–4021.
8. Singh, G.; Kumar, P. A.; Lundgren, C.; Helvoort, A. T. J. V.; Mathieu, R.; Wahlström, E.; Glomm, W. R. Particle & Particle Systems Characterization 2014, 31 (10), 1054–1059.

9. Herman, D. A. J.; Cheong-Tilley, S.; Mcgrath, A. J.; Mcvey, B. F. P.; Lein, M.; Tilley, R. D. Nanoscale 2015, 7 (14), 5951–5954.
10. Wani, I. A. Biomedical Engineering 1424–1447.
11. Wen, J. Z.; Goldsmith, C. F.; Ashcraft, R. W.; Green, W. H. The Journal of Physical Chemistry C 2007, 111 (15), 5677–5688.
12. Watt, J.; Bleier, G. C.; Austin, M. J.; Ivanov, S. A.; Huber, D. L. Nanoscale 2017, 9 (20), 6632–6637.
13. Huang, P.; Lin, J.; Li, Z.; Hu, H.; Wang, K.; Gao, G.; He, R.; Cui, D. Chemical Communications 2010, 46(26), 4800
14. Lacroix, L.-M.; Lachaize, S.; Falqui, A.; Respaud, M.; Chaudret, B. Journal of the American Chemical Society 2009, 131 (2), 549–557.
15. Hyeon, T.; Lee, J. Chemical Communications 2003, (8), 927-934.
16. Boles, M. A.; Ling, D.; Hyeon, T.; Talapin, D. V. Nature Materials 2016, 15 (3), 364–364.
17. Zhang, S.; Jiang, G.; Filsinger, G. T.; Wu, L.; Zhu, H.; Lee, J.; Wu, Z.; Sun, S. Nanoscale 2014, 6 (9), 4852–4856.
18. Kumara, L. S. R.; Sakata, O.; Kohara, S.; Yang, A.; Song, C.; Kusada, K.; Kobayashi, H.; Kitagawa, H. 2016.
19. Murray, C. B.; Kagan, C. R.; Bawendi, M. G. Annual Review of Materials Science 2000, 30 (1), 545–610.
20. Bai, Y.; Feng, J.; Wang, X.; Yin, Y.; Zhang, Q. Chemical Reviews 2016, 116 (18), 10983-11060.
21. Kim, D.; Park, J.; An, K.; Yang, N.-K.; Park, J.-G.; Hyeon, T. Journal of the American Chemical Society 2007, 129 (18), 5812–5813.
22. Slaton, R. D.; Bae, I.-T.; Lutz, P. S.; Pathade, L.; Maye, M. M. Journal of Materials Chemistry C 2015, 3(24), 6367–6375.
23. Gooch, J.; Jalan, A. A.; Jones, S.; Hine, C. R.; Alam, R.; Garai, S.; Maye, M. M.; Müller, A.; Zubieta, J. Journal of Colloid and Interface Science 2014, 432, 144–150.
24. Trunova, A. V.; Meckenstock, R.; Barsukov, I.; Hassel, C.; Margeat, O.; Spasova, M.; Lindner, J.; Farle, M. Journal of Applied Physics 2008, (9), 093904.
25. Lacroix, L.-M.; Huls, N. F.; Ho, D.; Sun, X.; Cheng, K.; Sun, S. Nano Letters 2011, 11 (4), 1641–1645.
26. Snoeck, E.; Gatel, C.; Lacroix, L. M.; Blon, T.; Carrey, J.; Respaud, M.; Lachaize, S.; Chaudret, B. EMC 2008 14th European Microscopy Congress 1–5 September 2008, Aachen, Germany 281–282.
27. Peng, S.; Wang, C.; Xie, J.; Sun, S. Journal of the American Chemical Society 2006, 128 (33), 10676–10677.
28. Bönnemann, H.; Brand, R. A.; Brijoux, W.; Hofstadt, H.-W.; Frerichs, M.; Kempter, V.; Maus-Friedrichs, W.; Matoussevitch, N.; Nagabhushana, K. S.; Voigts, F.; Caps, V. Applied Organometallic Chemistry 2005, 19 (6), 790–796.
29. Malvindi, M. A.; Greco, A.; Conversano, F.; Figuerola, A.; Corti, M.; Bonora, M.; Lascialfari, A.; Doumari, H. A.; Moscardina, M.; Cingolani, R.; Gigli, G.; Casciaro, S.; Pellegrino, T.; Ragusa, A. Advanced Functional Materials 2011, 2548.
30. Berlia, R.; Mk, P. K.; Srivastava, C. RSC Advances 2015, 5 (39), 30877–30881.
31. Gilroy, K. D.; Ruditskiy, A.; Peng, H.-C.; Qin, D.; Xia, Y. Chemical Reviews 2016, 116 (18), 10414–10472.

32. Teeriniemi, J.; Melander, M.; Lipasti, S.; Hatz, R.; Laasonen, K. The Journal of Physical Chemistry C2017, 121 (3), 1667–1674.
33. Wenjie, W.; Maye, M. M. Small 2013, 10 (2), 271-276.
34. Lutz, P.; Wenjie, W.; Maye, M. M. Abstracts of Papers of the American Chemical Society 2013, 246.
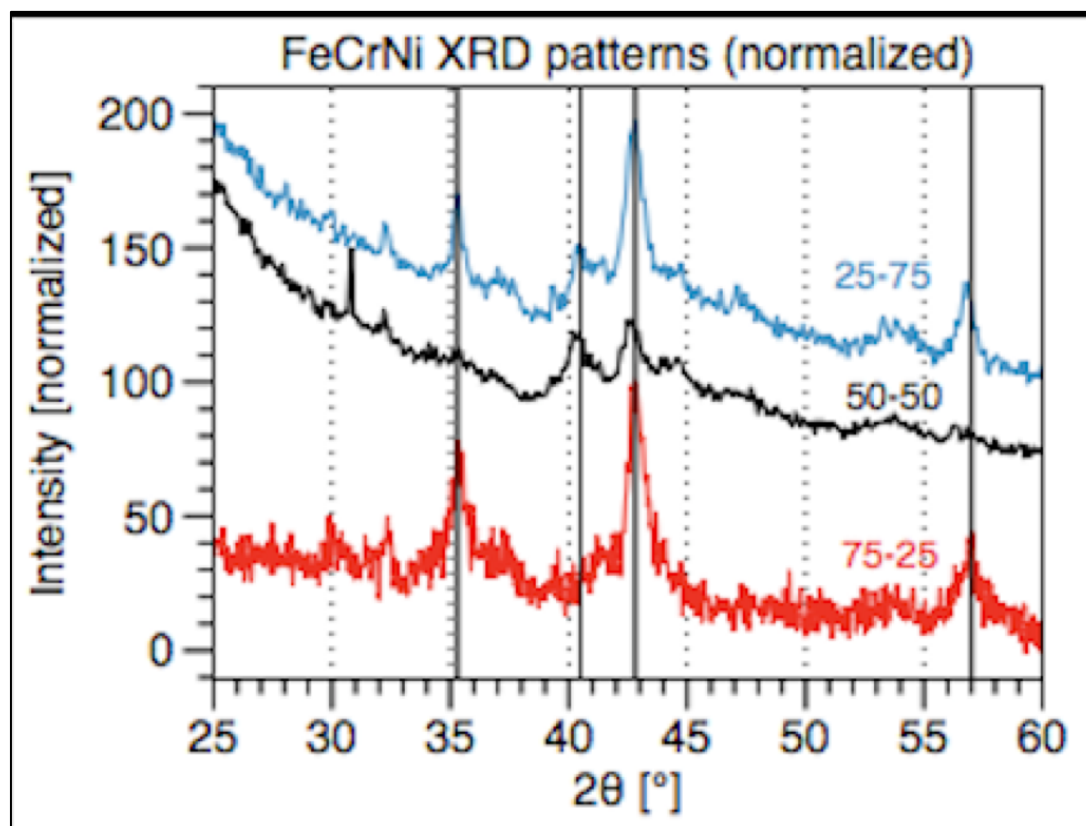
Appendices

Figure 1

Figure 7: XRD analysis of FeCrNi nanoparticles using iron core synthesized from $Fe(CO)_5$ (data from Dr. Mathew Maye)
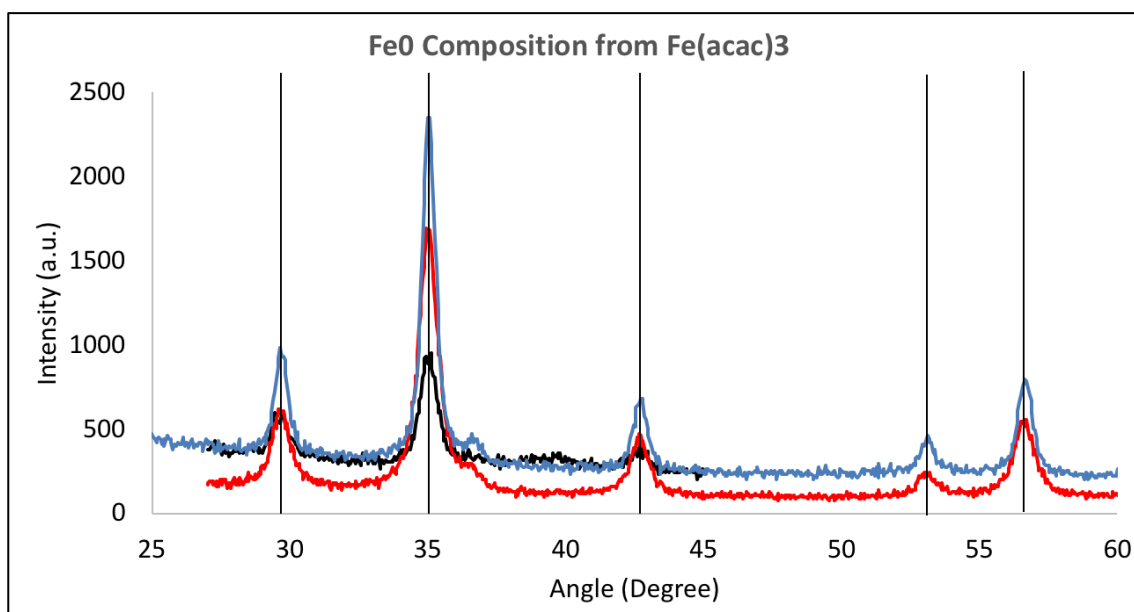
Figure 2

Figure 8: Fe⁰ nanoparticles synthesized from Fe(acac)3.

Figure 3
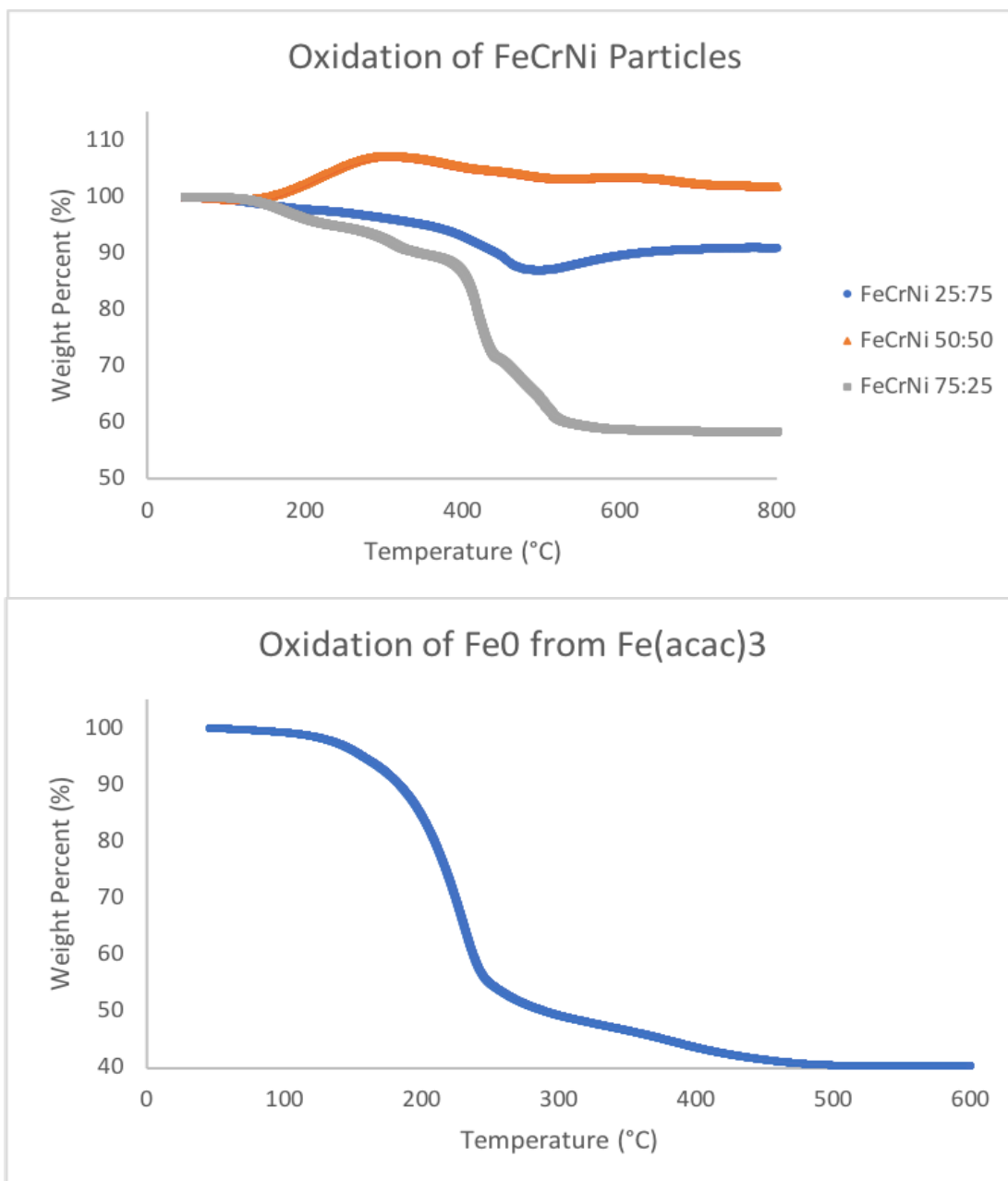
Figure 3: TGA of both a) FeCrNi particles synthesized using Fe_0 cores made from $Fe(CO)_5$ and b) Fe^0 particles synthesized using $Fe(acac)_3$
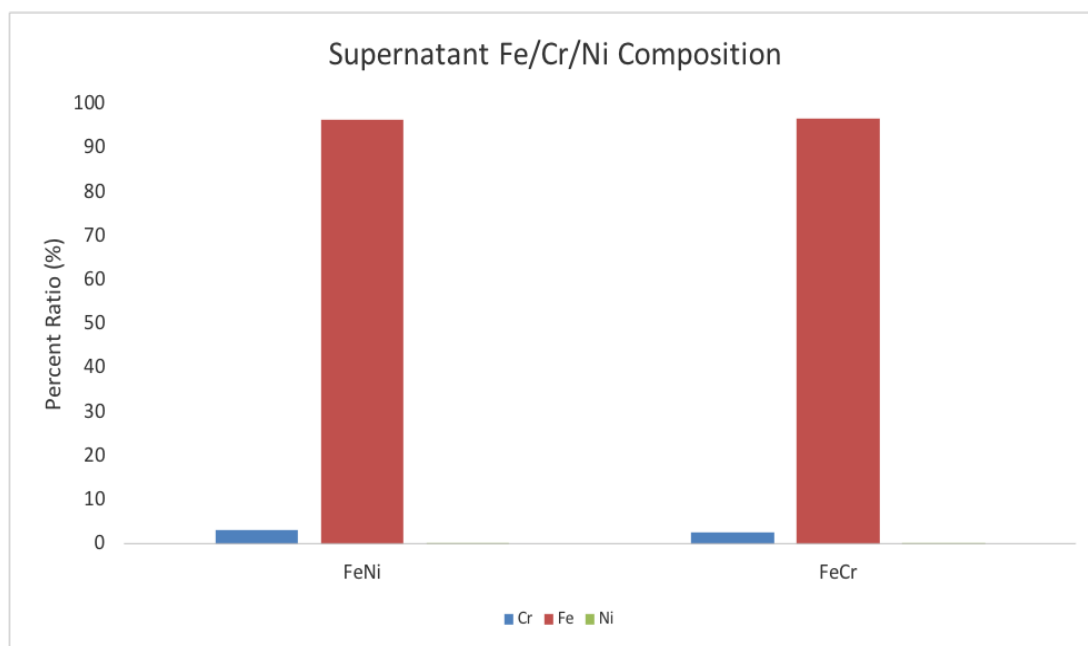
Figure 4

Figure 4: LA-ICP-MS data showing the amount of iron, nickel, and chromium in the supernatant of a reaction mixture for each respective particle
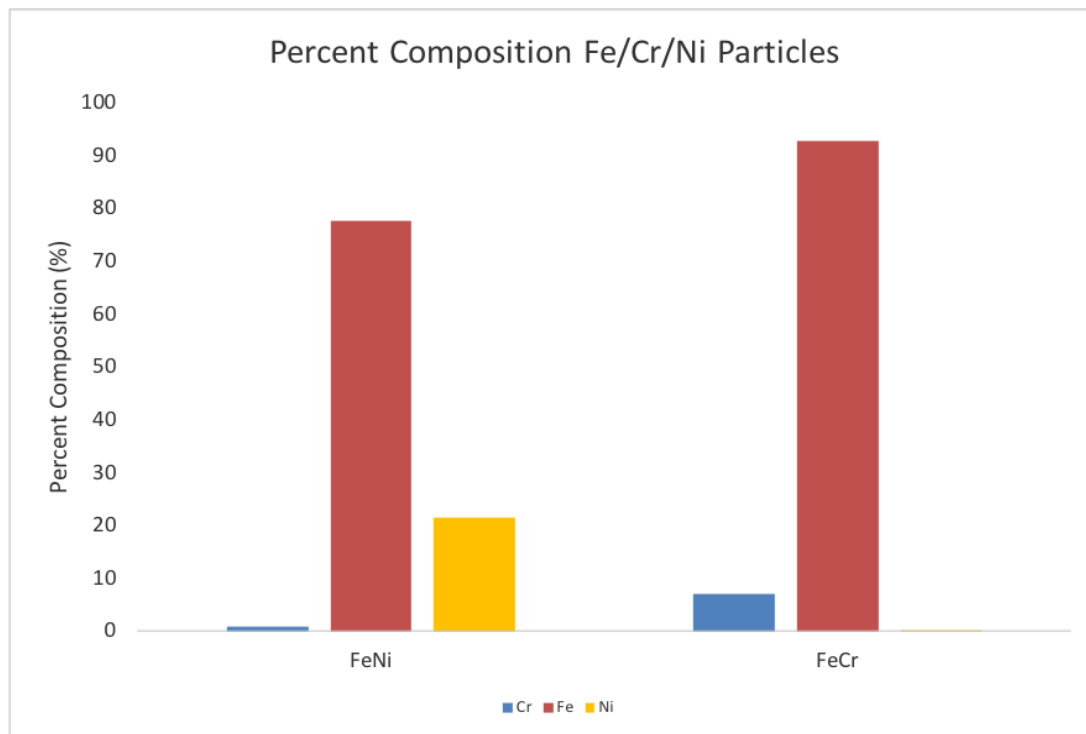
Figure 5

Figure 5: Analysis of FeNi and FeCr particles using LA-ICP-MS shows that each set of particles contained their respective core and shell materials
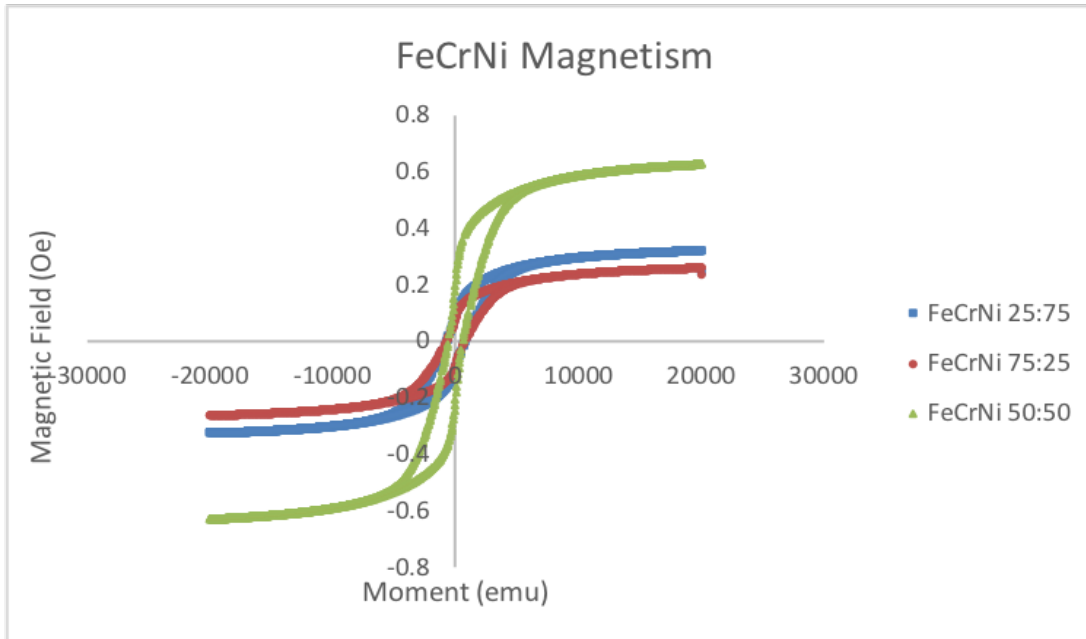
Figure 6

Figure 6: Magnetism data for three samples of FeCrNi particles with varying ratios of shell material